Environmental Science & Technology

Article

Cite This: Environ. Sci. Technol. 2017, 51, 12938-12947

pubs.acs.org/est

Water Footprint and Land Requirement of Solar Thermochemical Jet-Fuel Production

Christoph Falter*[,†] and Robert Pitz-Paal[‡]

[†]Bauhaus Luftfahrt e.V., Willy-Messerschmitt-Straße 1, 82024 Taufkirchen, Germany

[‡]DLR, Institute of Solar Research, Linder Höhe, 51147 Köln, Germany

ABSTRACT: The production of alternative fuels via the solar thermochemical pathway has the potential to provide supply security and to significantly reduce greenhouse gas emissions. H_2O and CO_2 are converted to liquid hydrocarbon fuels using concentrated solar energy mediated by redox reactions of a metal oxide. Because attractive production locations are in arid regions, the water footprint and the land requirement of this fuel production pathway are analyzed. The water footprint consists of 7.4 liters per liter of jet fuel of direct demand on-site and 42.4 liters per liter of jet fuel of indirect demand, where the dominant contributions are the mining of the rare earth oxide ceria, the manufacturing of the solar concentration infrastructure, and the cleaning of the mirrors. The area-specific productivity is found to be 33 362 liters per hectare per year of jet fuel equivalents, where the land coverage is mainly due to the concentration of solar energy for heat and electricity. The water footprint and the land requirement of the solar thermochemical fuel pathway are larger than the best power-to-liquid pathways but an order of magnitude lower than the best biomass-to-liquid pathways. For the production of solar thermochemical fuels arid regions are best-suited, and for biofuels regions of a moderate and humid climate.

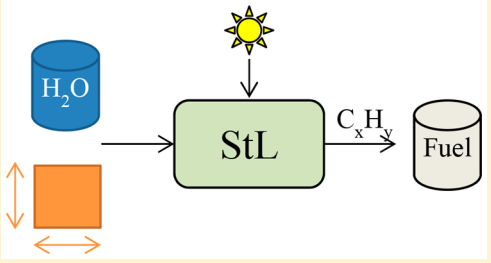

1. INTRODUCTION

Conventional fuels based on the refinement of crude oil remain by far the largest provider of energy to the transportation sector. However, concerns about their long-term availability, price stability, and climate impact have spurred the search for alternatives. While the electrification of cars appears to be an attractive option if costs can be decreased and if renewable energy can be used, the same solution cannot be implemented as easily in the aviation sector due to higher restrictions of the energy carrier in terms of energy density and specific energy.[1] The production of synthetic liquid hydrocarbon fuels presents a viable solution to reduce greenhouse gas emissions and to ensure supply security.[2] Several solutions have been proposed, e.g., fuels based on the conversion of biomass,[3,4] electrochemical fuels converting hydrogen derived by water electrolysis and CO derived from CO_2,[5] or the production of solar thermochemical fuels.[6] Among the different fuel options, the latter promise high energy-conversion efficiencies[7] and favorable greenhouse gas emissions.[2]

In the recent literature, the solar thermochemical fuel production pathway was analyzed with respect to its economic[2,8−10] and ecological performance including impact categories such as greenhouse gas emissions, acidification potential, or eutrophication potential.[2,11] It was found that the pathway has the potential for a significantly lower environmental impact at somewhat higher costs than the conventional fossil-based alternatives. The water consumption of solar thermochemical fuel production as well as its land requirement have not received detailed attention so far. Depending on the location of the fuel production, water demand or land requirement can, however, present serious issues with regard to the feasibility of the chosen production pathway. In particular, at the best plant locations in the arid regions of the Earth with high levels of direct irradiation and low humidity in the atmosphere, a lack of clean drinking water is the source of many diseases and conflicts. Climate change and the associated shortages of rainfall in some regions are expected to further worsen the situation, with 1.8 billion people living in regions with absolute water scarcity by 2025.[12,13] In these regions, the provision of water for fuel production may therefore be a challenge, and thus, it is of high importance to make sparingly use of freshwater resources. However, land availability is primarily a problem for biomass-based fuel production, as the best locations are in regions of high biodiversity, where competition with food production could arise. With the following analysis of water footprint and land requirement of solar thermochemical fuel production and its comparison with other alternative pathways, the discussion of alternative fuel options is sought to be complemented.

The solar thermochemical fuel pathway is based on the high-temperature conversion of water and carbon dioxide into a mixture of hydrogen and carbon monoxide (synthesis gas or syngas) and oxygen performed through cerium oxide (CeO_2 or ceria) redox reactions.[6,14] To attain the reduction temperatures of 1800 K and above that are normally required for redox

Received: May 22, 2017
Revised: September 21, 2017
Accepted: September 25, 2017
Published: September 25, 2017

DOI: 10.1021/acs.est.7b02633
Environ. Sci. Technol. 2017, 51, 12938−12947

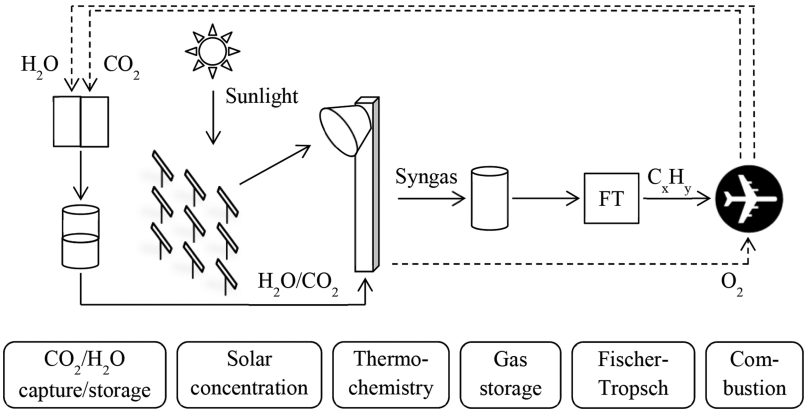

Figure 1. Schematic representation of the solar thermochemical fuel production path. H_2O and CO_2 are ubiquitous resources and can be captured from air or from the sea. Direct solar radiation is concentrated by a field of heliostats and enables the high-temperature thermochemical conversion of H_2O and CO_2 to H_2 and CO (syngas). The resulting syngas is stored and finally converted into jet fuel via the Fischer–Tropsch (FT) process.

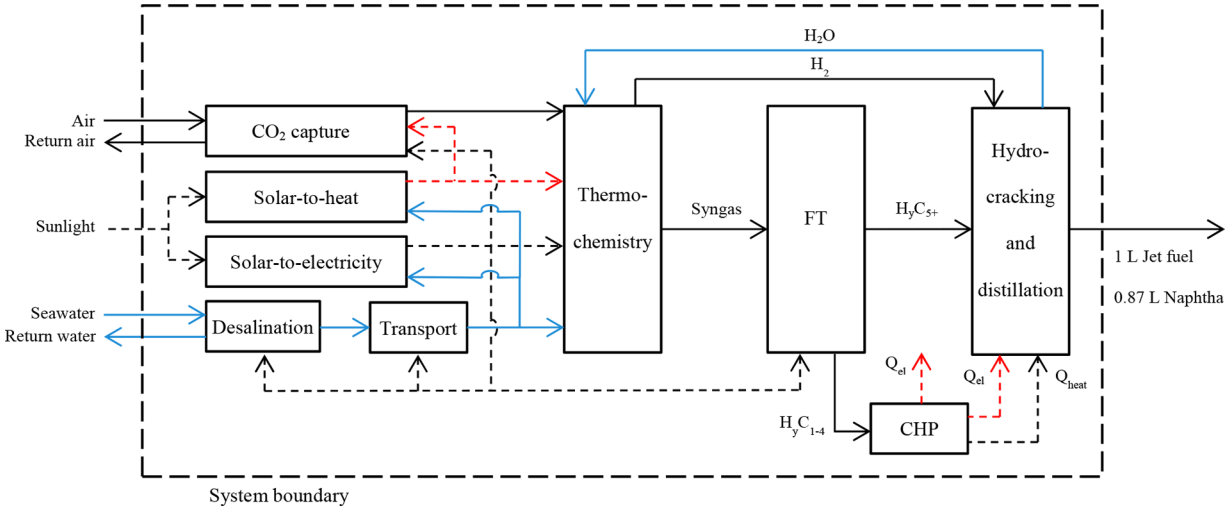

Figure 2. Process flowsheet of the baseline case of solar thermochemical fuel production as discussed in this study. CO_2 is captured from the air and H_2O is provided by seawater desalination and transported over 500 km distance and 500 m altitude to the plant. Electricity is provided by a concentrated solar power plant on site. Gaseous hydrocarbons are combusted in a combined heat and power (CHP) plant to provide heat and electricity to the process, while long-chained hydrocarbons are hydrocracked and distilled into the final products jet fuel and naphtha. Material flows are depicted with solid lines and energy flows with dashed lines.

reactions of metal oxides, solar energy is concentrated into a thermochemical reactor. The level of radiative flux can be reached with a solar tower or dish concentration system. Solar syngas is subsequently converted into liquid hydrocarbon fuels by the Fischer–Tropsch process. The resulting synthetic paraffinic kerosene is certified for commercial aviation in mixtures with a share of up to 50% with conventional jet fuel according to ASTM D7566.[15] A schematic representation of the cycle is shown in Figure 1.

The results presented in this paper apply to the following baseline case with a plant size of 1000 barrels per day (bpd) of jet-fuel production. As a co-product, 865 bpd of naphtha are produced from the same facility. The solar-stand alone facility, i.e. without external sources of heat or electricity, is located in a region with 2500 kWh m^{-2} $year^{-1}$ of direct normal irradiation where the concentration facility is a tower system. Thermochemical conversion efficiency is 20%, which is well within the thermodynamic limit. CO_2 is supplied by an air capture unit located at the plant site and H_2O by a seawater desalination unit located at 500 km distance and 500 m altitude difference, where it is assumed that an existing pipeline can be used for transport. The provision of water by seawater desalination is a conservative estimate, as water is captured concurrently with CO_2 from the atmosphere and could theoretically satisfy the demand, depending on the local temperature and relative humidity. The results would only be slightly affected; however, as the electricity demand for desalination and water transport is very small. Other system specifications can be taken from ref 2. A detailed process flowsheet is shown in Figure 2. To illustrate the size of the baseline case plant, the areas of the system components are shown in Figure 3.

For the concentrator, an optical efficiency of 51.7% is assumed,[16] and for the concentrated solar power (CSP) plant, a solar-to-electricity conversion efficiency of 20%, each with a land coverage factor of 25%. For CO_2 capture, 4.7 m^2 are required for the capture of 50 tons $year^{-1}$.[17] The size of the gas-to-liquid facility is assumed to be equal to the buildings required for a solar thermochemical hydrogen generation plant.[10] The largest area is required for the concentration of solar energy (26.1 km^2), followed by the production of solar electricity (5.3 km^2). The other components only use a comparably small area.

DOI: 10.1021/acs.est.7b02633
Environ. Sci. Technol. 2017, 51, 12938–12947

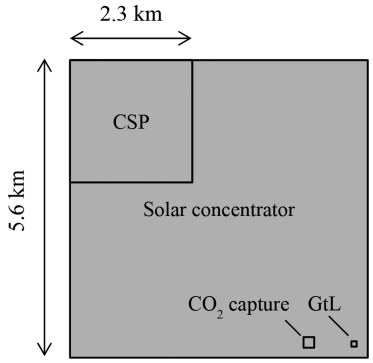

Figure 3. Schematic illustration of baseline case plant area. The total covered area is 31.4 km^2, where the largest shares are due to the solar collector with 26.1 km^2 and the concentrated solar power (CSP) plant with 5.3 km^2. The CO_2 capture plant, the gas-to-liquid facility (GtL), and the storage of syngas (not visible) only require small areas and are assumed to fit in the open spaces of the solar concentrator.

The major part of the materials used are composed of steel, concrete, alumina, glass, and ceria. Required amounts of these materials are listed in Table 1, where the values are estimates only because exact data were not always available, and in the calculations in some cases, aggregated specific values of the material requirements were used. The material demand for the heliostat field is based on ref 18 and the one for the tower is a conservative estimate, assuming an increase in material requirement proportional to the increase of field size.[19] The material demand for the solar reactors is estimated based on laboratory experiments,[6] that of the CSP plant is from a recent study,[19] the one for CO_2 capture is from a rough estimate of existing collectors,[17] and that for the gas-to-liquid component is derived from values for the Pearl GtL plant in Qatar.[20]

2. METHODS

2.1. Water Footprint. *2.1.1. Goal and Scope.* The goal of the analysis performed here is the estimation of the direct and indirect water footprint and the land requirements associated with the production of solar jet fuel and naphtha. The functional unit is chosen to be one liter of jet fuel and 0.87 L of naphtha, which is produced as a byproduct in the same process.[21] A well-to-wake boundary is defined that includes provision of resources, concentration of solar energy, thermochemistry, and the Fischer−Tropsch conversion. The life cycle phases of construction, manufacturing, and disassembly are taken into account for the plant components. The construction of the seawater desalination plant is neglected as its contribution is estimated to be well below a limit of 1% of the overall water footprint.[22] The infrastructure requirement for the CO_2 capture plant is estimated from published values of demonstration plants,[17] where it is found that the contribution of the capture plant infrastructure is below 1% of the total water footprint and is neglected. Other environmentally friendly sources of CO_2 are biogenic point sources such as ethanol plants, where the impact on the results for a change to these sources is expected to be small. The provision of CO_2 from fossil point sources, however, strongly deteriorates the life cycle emissions of the process.[2] In the case of the FT unit, the water footprint associated with the construction of the facility was estimated based on material requirements of a large-scale GtL plant in Qatar, and it was found that the contribution was also well below 1% of the overall water footprint. The water demand for the transport of the materials to the plant location and the deconstruction are not assumed to exceed that of the manufacturing phase and are neglected except for the main infrastructure component of the solar concentration field.

2.1.2. System Description and Inventory Analysis. A distinction is made between direct and indirect water use.[23] The former is characterized by water consumption directly at the plant site and is required for operation, e.g., the cleaning of mirrors. The latter is water that is used in other parts of the world, mainly to produce the materials and plant components, e.g., the production of steel and the subsequent manufacturing of heliostat frames. Depending on the material intensity and the types of materials used, the indirect water demand can surpass the direct water demand, while the latter is usually the main focus of attention. To avoid the miscalculation of the total water footprint of the production of solar thermochemical fuels, both direct and indirect water demand are analyzed in this study. In the following, the origins of water consumption are identified throughout the production process and the respective values are indicated that serve as a basis for the calculation of the water footprint. The contributions to the indirect water demand are listed and explained below. The results are normalized to the amount of product (jet fuel or naphtha) with an allocation between the products based on their energy content (lower heating value).

Solar energy is concentrated with a heliostat field onto a receiver on top of a tower. The heliostats consist mainly of a foundation holding a steel frame with a mirror structure made from a coated glass, and gear drives that perform two-axis tracking to maintain the reflected radiation on the target. The tower consists of a steel and concrete structure holding in place the receivers and providing space for operation and maintenance. A recent study[19] analyzing the greenhouse gas emissions and water consumption of a concentrated solar power (CSP) plant with thermal energy storage in a two-tank molten salt system is used as a reference to derive the water demand for the construction of the solar concentration system. The indicated value of 0.22 L kWh_{el}^{-1} is converted to the basis of unit area of reflective surface using the properties of the reference plant, giving 2848 L m^2 for the manufacturing, construction, dismantling, and disposal of the heliostats. Equally, the water demand for the same life cycle phases of

Table 1. Estimated Amounts of Materials Used for Baseline Case Plant

	steel (kg)	concrete (kg)	alumina (kg)	glass (kg)	ceria (kg)
heliostat field	1.76×10^8	–	–	6.62×10^7	–
tower	–	3.59×10^8	–	–	–
solar reactors	1.05×10^7	–	3.49×10^6	2.09×10^6	6.98×10^6
CSP	5.55×10^7	2.05×10^8	–	1.37×10^7	–
CO_2 capture	1.30×10^7	–	–	–	–
GTL	1.07×10^6	6.39×10^6	–	–	–

DOI: 10.1021/acs.est.7b02633
Environ. Sci. Technol. 2017, 51, 12938−12947

the tower is derived assuming linear scaling with the thermal power input, giving 381 L m^2 of reflective surface area. The total water demand of the solar concentration system is then calculated by multiplying the total reflective surface area of 6.53 × 10^6 m^2 with the sum of the specific water demands, giving 2.11 × 10^{10} L. Normalizing to the amount of fuel produced from the plant with a capacity of 1000 bpd of jet fuel and 865 bpd of naphtha over the assumed lifetime of 25 years, 8.1 liters per liter of jet fuel are required for the manufacturing, construction, dismantling and disposal of the tower and heliostat field.

Concentrated solar energy enters the reactors and drives a redox cycle of a metal oxide assumed here to be ceria. The water demand for the manufacturing of the solar reactors is estimated from the amount of used materials, i.e. steel, alumina, glass, and ceria, which are multiplied with the respective impact factors for the production of the materials. Construction and transport of the materials is neglected because these phases were observed to have very little impact on the result.[19] The amount of the materials used is estimated from experiments with a ceria reactor,[6] assuming linear scaling with the thermal input power. The accuracy of this approach to determine the amount of materials is difficult to judge as no technical implementation on a much larger scale has been seen so far. However, the required amount of ceria can be accurately determined based on the assumptions made about the reaction conditions, i.e. a nonstoichiometry of 0.1 at 16 cycles per day. For the indicated number of cycles, which corresponds to experimentally shown values,[24] this requires oxygen partial pressures of 10^{-3}−10^{-4} atm at reduction temperatures of above 1900 K. From the experimental values achieved today, this presents a challenge. However, if cycle times can be further reduced, the requirements for the achieved nonstoichiometry per cycle are relaxed. Compared to the water footprint of ceria, that of the manufacturing of the reactor structure has a negligible impact. The required amount of materials for the thermochemical reaction step are 0.39 kilograms of steel, 0.13 kilograms of alumina, 0.08 kilograms of glass, and 0.26 kilograms of ceria per kW_{th}, where these values are estimated from recent experiments.[6,25] While, however, the specific water demands for the production of steel, alumina, glass, or concrete are smaller than 15 L kg^{-1},[26] the value rises to 11 830 L kg^{-1} for ceria from the mining in the Bayan Obo mine in China, which supplies the majority of the world's production.[27] At this location, rare earths appear together with hematite and columbite in the form of bastnasites and monazites. During mining and beneficiation, the minerals are taken from the mine and separated from hematite and columbite. In the next step, the light, medium, and heavy oxide groups of rare earths are purified and separated using cracking, acid leaching, impurity removal, and precipitation. The single rare earth oxides can then be singled out in a multistage acidic extraction process.[27] Water is required for the production and use of the chemicals used for the separation processes as well as for the energy inputs. A similar value of about 7500 L kg^{-1} of cerium (reduced from the oxide) is reported in ref 28, while a much-lower value of 300 L kg^{-1} is indicated in a sample case study using bastnasite only in ref 29. Because the studies indicating the higher values are more suitable for the chosen source of material and to pick a conservative value, 11 830 L kg^{-1} of cerium oxide is chosen. As can be seen from the results below, even the assumption of this value does not lead to a prohibitive water demand. The resulting impact of the manufacturing of the thermochemical reactors is therefore clearly dominated by the reactive material ceria. The impact of the remaining reactor materials is negligible.

The electricity demands are covered by a CSP tower plant, which is assumed to be built next to the thermochemical plant. Because the electricity production works on the principle of concentration of solar energy, its conversion to heat and, finally, the transformation of heat into electricity, the material requirements for the concentration of solar energy are similar to the solar concentration of the thermochemical plant and are indicated to be 0.43 L kWh_{el}^{-1}[19] for the construction of the CSP plant, which is equal to 7.1 L per functional unit or 2.7 liters per liter of jet fuel produced over the lifetime of the plant.

The material requirements for the construction of the Fischer−Tropsch unit are estimated by scaling those of the large-scale Pearl GtL plant in Qatar linearly from 140 000 bpd of liquid fuels to 1865 bpd of the thermochemical fuel production plant.[20] The water demand for steel and concrete are then 1.32 × 10^7 L or 5.03 × 10^{-3} liters per liter of jet fuel.

The direct water demand associated with the operation of the fuel production plant at the designated location consists of the following contributions. Because sand and dirt accumulate with time on the heliostats, a cleaning procedure is required to maintain a high reflectivity. Different values for the water demand of the cleaning have been published, whereas here, 58.0 L m^{-2} $year^{-1}$ indicated in a recent life cycle analysis of a tower CSP plant[19] are used. For the solar thermochemical fuel plant, this corresponds to 6.5 L per functional unit or 3.62 liters per liter of jet fuel. The authors state that for the Ivanpah CSP plant, water consumption for cleaning is reported to be three times smaller than this estimate, which appears to be conservative. The water demand could be further reduced through the filtration of the cleaning water, which is, however, not further pursued at this point.

For the production of one functional unit, the Fischer−Tropsch unit receives 395.2 mol of syngas as input, which requires 267.7 mol of hydrogen and additionally 13.3 mol of hydrogen for hydrocracking. Assuming complete conversion of water into hydrogen and oxygen, 5.1 L of water have to be supplied to the thermochemical reaction. In the FT synthesis, 2.1 L of water are produced that can be recycled, reducing the required water input for thermochemical conversion to 3.0 L. This corresponds to 1.7 L L^{-1} jet fuel.

For the production of solar thermochemical fuels, electricity is required for the purification of inert gases (80% of total electricity requirement), for CO_2 capture (10%), for the FT synthesis (6%), for the separation of CO and CO_2 coming out of the thermochemical reactors (3%), and for the desalination and transport of water (2%). The production of inert gases requires 16 kJ_{el} mol^{-1}[30] by cryogenic rectification, whereas alternatively, the operation of the plant under vacuum with reduced amounts of inert gases is suggested. Carbon dioxide is assumed to be captured from the atmosphere by chemical adsorption[31−33] to an amine-functionalized solid sorbent with an energy requirement of 1500 kWh of low-temperature heat and 200 kWh of electricity per ton.[34] The impact of water desalination is very small and therefore not sensitive to the capture technology used.

The syngas coming from the solar reactors has to be pressurized to the pressure of the FT synthesis of 30 bar, which requires 4.2 MJ of electricity, 2.3 MJ of which are supplied by conversion of solar primary energy and 1.9 MJ are supplied from internal conversion of intermediate products.[2] Hydro-

DOI: 10.1021/acs.est.7b02633
Environ. Sci. Technol. 2017, 51, 12938−12947

cracking and distillation reduces the chain lengths of the hydrocarbons to the desired ranges, separates the products and has energy demands of 0.3 MJ_{el} of electricity and of 1.9 MJ of heat,[35] both of which are supplied from the combined heat and power unit combusting the light hydrocarbon fraction of the FT conversion. As an environmentally and potentially economically attractive alternative, the light hydrocarbons could be reformed into syngas and cycled back to the FT unit. Here, however, the conversion of the light hydrocarbons in a CHP plant is assumed as this is also close to the current practice of GtL plants. Due to kinetic and thermodynamic reasons, CO_2 is supplied in excess to the thermochemical reaction, resulting in a mixture of CO and CO_2 at the exit of the reactors. To recycle the unreacted CO_2 and to improve the gas mixture for the FT synthesis, the gas components are separated by selective binding of the CO_2 to a liquid sorbent, as is commonly suggested for the post-combustion capture of CO_2 from fossil power plants. The energy requirements are 132 kJ mol^{-1} of heat and 9 kJ_{el} mol^{-1} of electricity.[36] Fresh water for the process is provided through seawater desalination and the subsequent transport of the water over a 500 km distance and 500 m altitude difference to the fuel plant. Desalination can be accomplished with methods based on thermal separation or membrane separation, where the latter has smaller energy demands of 3 kWh_{el} m^{-3} or 10.8 kJ L^{-1} and is selected here. The pump energy for the designated distance and altitude difference is calculated with information from ref 37, resulting in 38.6 kJ L^{-1}. In total, for the generation of CSP electricity on-site, 3.9 L of water is used for the production of one functional unit or 2.1 liters per liter of jet fuel, whereas most of the water is consumed for the steam cycle, the balance of the plant, and the heliostat cleaning.

2.2. Land Requirements. Land requirement is defined as the total area of land used for the production of a defined amount of jet fuel. This metric can be used to compare different fuel production pathways like unconventional fuel production, biofuels, or other alternatives. A smaller land requirement is advantageous because the environmental and social impact will be reduced. However, the plant location is also very important because a plant construction in a desert region is likely to have a much smaller impact on the environment and the regional population than a construction in areas of large population density and rich flora and fauna. In the metric of land requirement this is not reflected. In addition, the quality of the land coverage is decisive: while biological plants are perceived to be a more natural environment, industrial facilities may be seen as more critical.

When the system boundaries for different fuel paths are chosen in such a way that primary solar energy, CO_2, and H_2O are utilized for jet fuel production, land requirement is directly related to the system efficiency as the latter describes how well the primary solar energy is converted into the product. For a lower efficiency, more land is required to supply the primary energy for the conversion into the same amount of product. The reference area of the solar thermochemical efficiency is the reflective area of the mirrors. To derive the total covered land area of the facility, a land coverage factor has to be defined. In the case of concentrated solar tower plants, this factor is around 25%,[38] i.e., the total covered land area is four times the reflective area of the mirrors. The area requirement for the solar tower and the fuel conversion plant is neglected because it covers a small area compared to the heliostat field and may be placed in between the mirrors.

The land requirement $A_{\text{total ground}}$ of the solar thermochemical process is thus calculated:

$$A_{\text{total ground}} = \frac{N_{\text{fuel,daily}} \cdot 365 \frac{\text{days}}{\text{year}} \cdot \text{LHV}_{\text{jet fuel}}}{\text{DNI}_{\text{annual}} \cdot \eta_{\text{land coverage}} \cdot \eta_{\text{solar-to-jet fuel}}} \quad (1)$$

$\text{DNI}_{\text{annual}}$ is the annual direct normal irradiation per unit area at the plant location, $\eta_{\text{solar-to-jet fuel}}$ is the energy conversion efficiency of solar primary energy to jet fuel [$\eta_{\text{solar-to-jet fuel}}$ is equal to 55.4% of the overall energy conversion efficiency from sunlight to 1 L of jet fuel and 0.87 L of naphtha based on an energy allocation (LHV)], $\eta_{\text{land coverage}}$ is the land coverage factor (assumed to be 25%), $N_{\text{fuel,daily}}$ is the daily jet fuel production from the plant in liters, and $\text{LHV}_{\text{jet fuel}}$ is the lower heating value of jet fuel (33.4 MJ L^{-1}).[4]

3. RESULTS

3.1. Water Footprint. In total, the direct water footprint is 13.4 L of water per functional unit or 7.4 liters per liter of jet fuel and the indirect water footprint is 76.5 L per functional unit or 42.4 liters per liter of jet fuel. The contributions to both the direct and indirect water footprint are shown in Tables 2 and 3 and Figures 4 and 5.

Table 2. Overall Direct Water Footprint for the Production of Solar Thermochemical Jet Fuel

	liters per liter of jet fuel	liters per liter of naphtha	liters per functional unit
mirror cleaning	3.62	3.37	6.54
thermochemistry	1.66	1.54	2.99
electricity	2.14	1.99	3.86
total	**7.41**	**6.90**	**13.39**

Table 3. Overall Indirect Water Footprint for the Production of Solar Thermochemical Jet Fuel

	liters per liter of jet fuel	liters per liter of naphtha	liters per functional unit
solar concentration infrastructure			
heliostats	7.10	6.61	12.83
tower	0.95	0.89	1.72
thermochemistry			
ceria	31.5	29.4	56.9
alumina	0.0031	0.0029	0.0055
steel	0.043	0.040	0.078
glass	0.011	0.010	0.020
CSP infrastructure	2.70	2.52	4.88
Fischer–Tropsch infrastructure			
steel	0.0044	0.0041	0.0080
concrete	0.00062	0.00057	0.0011
total	**42.4**	**39.4**	**76.5**

The overall water footprint is dominated by the indirect contributions, which are responsible for more than five times the amount of the water used on-site. Ceria mining has a relative weight of 75% of the indirect water use, followed by the water demand of the heliostat field with 17% and for the CSP facility with 6%. The other items only have minor contributions. The single largest contributor to the water demand is therefore the provision of the rare earth oxide ceria, which is currently almost exclusively provided by China. If solar thermochemical fuels or other technologies should lead to a

DOI: 10.1021/acs.est.7b02633
Environ. Sci. Technol. 2017, 51, 12938−12947

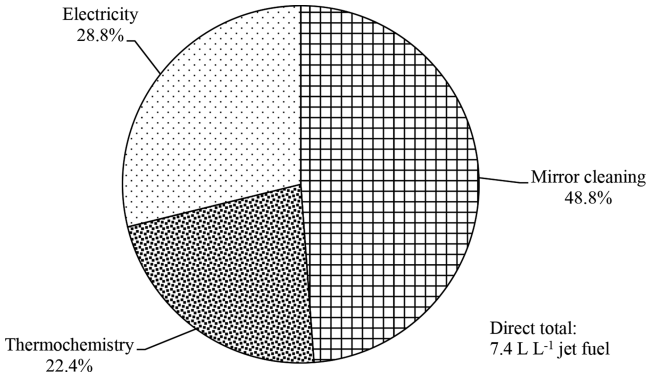

Figure 4. Contributions to overall direct water footprint in the baseline case of the solar thermochemical fuel production plant.

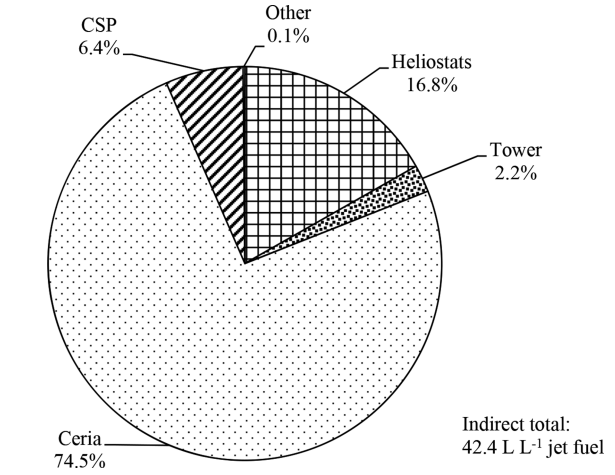

Figure 5. Contributions to overall indirect water footprint in the baseline case of the solar thermochemical fuel production plant.

significant increase in the demand for rare earth oxides, it is conceivable that other mines will be opened. Because the mining step is a crucial input for this process but also for others, a reduction of the water demand should be targeted. Water is required during the mining and beneficiation stages for wet-magnetic separation and froth flotation, during the purification and separation stages for water leaching, and during the multistage extraction processes to separate the individual rare earth oxides by extraction, scrubbing, and stripping, besides others.[27] If ceria is replaced by a reactive material with a low specific water demand (such as Fe_3O_4 or ZnO), the water footprint of solar fuel production can be decreased from 49.8 to about 18 L_{H_2O} L^{-1} of jet fuel.

About half of the direct water footprint is due to cleaning of the heliostat surfaces and about a quarter each for the production of CSP electricity (which also requires water for mirror cleaning) and for thermochemistry. As can be expected from an efficient chemical process, the water demand for the actual synthesis of the fuels is on the order of the volume of the produced fuels and small compared to the overall water footprint. The direct water footprint is about four times higher than the minimally required water input to the chemical synthesis and could be reduced by a CSP plant using less water than the assumed value here through a dry-cooled cycle and possibly more efficient cleaning procedures for the mirror surfaces. The Ivanpah power plant, for example, is reported to use significantly less water for cleaning and the steam cycle.[19]

The overall water footprint is then the sum of the indirect and the direct contributions and has a value of 89.9 L per functional unit or 49.8 liter per liter of jet fuel.

In the following, the total water requirements of fuel production pathways based on conventional jet fuel production, conversion from oil sands and oil shale, coal-to-liquids, gas-to-liquids, different biofuels, power-to-liquids (PtL), and solar thermochemistry are compared. In Table 4, an overview of the water footprints of the chosen fuel pathways is shown. The lowest water footprint is achieved for the fossil-based fuel pathways. In case of conventional jet fuel production, only a small amount of water is required for the recovery of the crude oil from underground and for its refining into the final products. Enhanced oil recovery may increase the water footprint significantly if water is pressurized to recover a higher share of the crude oil trapped underground. The processing of Canadian oil sands does not require a larger amount of water than conventional fuel production, while the gas- and coal-to-liquid processes may have a somewhat larger impact on the water resources, depending partly on the chosen technologies and, in the case of the coal-to-liquid process, also on the water content of the coal. The biomass-based pathways have a higher water footprint by 3 orders of magnitude compared to the fossil-based pathways, where the overall values are a combination of blue, green, and gray water demand. This is due to the large amount of water that is required to irrigate the feedstock and the water lost through evaporation and transpiration from the plant, while in the case of the fossil fuels, the feedstock already contains carbon or even hydrocarbons and can more easily be transferred into the final product. Among the biomass-based pathways, biodiesel from biomass has a larger water footprint than ethanol, while biodiesel from microalgae is in the same overall range as ethanol. All other water footprints are assumed to be based on blue water. To derive the water footprint of the PtL pathways, an energy-conversion efficiency from electricity to FT products of 44.6% is assumed,[39] where the water intensity of electrical energy generation from different sources is taken from ref 40. Additionally, a water input of 226.3 mol per liter of jet fuel is required to produce hydrogen, which is partly reacted with CO_2 in a reverse water gas shift reaction to generate CO for the FT conversion, and partly used for hydrocracking of the FT products.[2] For the solar thermochemical fuel pathway, a range of 7−50 liter of water per liter of jet fuel is derived from the calculations in this chapter, where the lower value corresponds only to the direct water demand on-site and the higher value corresponds to the fuel life cycle water footprint including direct and indirect consumption. For comparison with the other fuel pathways, the lower value is chosen because, commonly, only the on-site operational requirements are taken into account.

The solar thermochemical pathway therefore has a similar water footprint compared to the fossil-based options and one that is lower by orders of magnitude than the biomass-based options. Even the consideration of the higher value of the solar thermochemical fuel pathway or a significant change in the assumptions (see section 4) does not change this result. However, the water demand for biofuels occurs mainly in less arid regions and may therefore be less critical. Nevertheless, the large water footprint of biofuels may have a negative impact on their feasibility and large-scale scalability. Compared to the competing power-to-liquid pathway based on water electrolysis, reverse water gas shift, and Fischer−Tropsch synthesis, the

DOI: 10.1021/acs.est.7b02633
Environ. Sci. Technol. 2017, 51, 12938−12947

Table 4. Overview of Water Footprints of Different Fuel Production Pathways in Liters of Water per Liters of Product (Gasoline, Jet Fuel, Ethanol, Biodiesel, and FT Liquids) and Converted to the Common Metric of Liters of Jet Fuel, in Which the Conversion Is Based on Lower Heating-Value Equivalents[a]

fuel pathway	water footprint (L L^{-1})	water footprint (liters per liter of jet fuel)	source
conventional gasoline[b]	1−3	1−3	U.S. Department of Energy[41]
(U.S. conventional crude)	3−7	3−7	Wu et al.[42]
Canadian oil sands (gasoline)[b]	3−6	3−6	Wu et al.[42]
enhanced oil recovery	2−350	2−350	U.S. Department of Energy[41]
coal-to-liquid (FT liquid)[c]	5−7	5−7	U.S. Department of Energy[41]
coal-to-liquid (jet fuel)	10−60	10−60	Vera-Morales et al.[43]
gas-to-liquid (jet fuel)[e]	2−7	2−7	Vera-Morales et al.[43]
ethanol from biomass	≥1000[f]	≥1582	Dominguez-Faus et al.[44]
	1200−7000[g]	1899−11075	Mekonnen et al.[45]
	420−4254[h]	665−6731	Gerbens-Leenes et al.[46]
	1380[i]	2183	U.S. Department of Energy[41]
biodiesel	5150−18150[g]	5274−18586	Mekonnen et al.[45]
	7521−11636[h]	7702−11916	Gerbens-Leenes et al.[46]
	5625[i]	5760	U.S. Department of Energy[41]
biodiesel from microalgae	591−3650[j]	605−3738	Yang et al.[47]
	1000−9000	1024−9216	Vera-Morales et al.[43]
PtL−wind power	4−5	4−5	Mekonnen et al.[40]
PtL−Photovoltaic (PV)	5−31	5−31	Mekonnen et al.[40]
PtL−CSP	28−438	28−438	Mekonnen et al.[40]
PtL−coal	10−162	10−162	Mekonnen et al.[40]
solar thermochemical	7−50[k]	7−50	this study

[a]The calculated water footprint for the solar thermochemical fuel pathway is low compared to biofuel pathways. The lowest footprint is achieved for the fossil fuel pathways because of the low water intensity of the involved process steps. The LHVs used for the conversion to the common basis of liter of jet fuel are jet fuel 33.4 MJ L^{-1},[4] gasoline 32.2 MJ L^{-1},[48] biodiesel 32.6 MJ L^{-1},[48] and ethanol 21.1 MJ L^{-1}.[48] [b]Values include exploration, production, and refining. [c]The range of values depends on the origin and the water content of coal. [d]Includes coal mining and washing and coal-to-liquids conversion. [e]Includes only the gas-to-liquid conversion process. [f]Includes irrigation and evapotranspiration for a range of different feedstock. [g]Global average value that includes green, blue, and gray water for a range of different feedstock. [h]Total-weighted global average value that includes green and blue water for a range of different feedstock. [i]Irrigation water based on a survey of the USDA. [j]Value depends on water recycle rate. [k]The lower value includes only on-site consumption; the higher value also includes off-site consumption.

direct water footprint is expected to be about equal. The reason for this is an efficient chemical hydrocarbon synthesis that does not include biomass-based plant growth with the associated losses of evapotranspiration. Additionally, water is required for cleaning the mirrors or PV modules and for electricity taken from different sources such as coal, CSP, PV, or wind. A more detailed analysis for the power-to-liquid pathway is needed to clarify the water requirements associated with the materials of the electrolyzer.

Even though the water footprint of solar thermochemical fuels is identified to be comparably small, the provision of water at the best suited plant locations in the desert regions could present a challenge. In the baseline case of the fuel production facility, water is assumed to be supplied by seawater desalination and transported over a 500 km distance and 500 m altitude difference.[2] Assuming the use of an existing pipeline, the impact on the economical and ecological performance of the process is negligible. Alternatively, water can be captured from the atmosphere as a byproduct of CO_2 air capture[31] because even in desert regions, the water content in air is higher than the CO_2 content (by mass). This would obviate the pipeline needed for the transport of desalinated water. However, even when the costs of the pipeline are included, the economics of the overall process are not expected to be significantly disturbed.

3.2. Land Requirements. Overall, 1.22 GJ of solar primary energy are captured and converted into the intermediates heat and electricity with efficiencies of 51.7%[16] and 20.0%, respectively, producing 1 liter of jet fuel and 0.87 liter of naphtha. The overall energy conversion efficiency based on the LHV of jet fuel and naphtha is thus (1 L × 33.4 MJ L^{-1} + 0.87 L × 31.1 MJ L^{-1})/1.22 GJ = 5.0%. This value includes the provision of heat and electricity used in the process. While in other publications, higher numbers are mentioned for the overall efficiency, our more conservative estimate is based on a thermochemical efficiency of 20%, which is well below the thermodynamic limit. At experimental values that are at about 5% today,[24] the achievement of 20% seems to be an ambitious but realistic target for the midterm future and was therefore selected here.

Using eq 1 for the facility with a total jet fuel production of 1000 bpd (and 865 bpd naphtha) located in a favorable region with a solar irradiation of 2500 kWh m^{-2} $year^{-1}$ and an efficiency of 5.0% gives an area of 31.40 km^2, i.e. a square with a length of about 5.6 km (Figure 3). The corresponding annual production per hectare is 18 480 liters of jet fuel and 15 985 liters of naphtha or 1.85 liters of jet fuel and 1.60 liters of naphtha per square meter per year. Considering different assumptions about efficiency, these values compare well with the previous findings of 5.8 liters of jet fuel equivalent per square meter and year.[11]

The land requirement of the solar thermochemical fuel pathway is compared with other pathways, i.e. the biomass-to-liquid pathway (BtL, i.e. gasification of biomass and FT conversion of the syngas), hydroprocessed ester and fatty acids (HEFA, i.e. hydroprocessed of native fat or oil and subsequent refining), and power-to-liquid (PtL, production of hydrogen by water electrolysis, reverse water gas shift, and FT conversion).

DOI: 10.1021/acs.est.7b02633
Environ. Sci. Technol. 2017, 51, 12938−12947

First, the land requirements of several biomass-based pathways are taken from the literature. In ref 49, the productivity of 18 different plants is derived in a rigorous analysis based on high-resolution geometric data. The maximum productivity under ideal circumstances for plant growth is found to be 5812 liters of jet fuel-equivalents per hectare and year for oil palms with the HEFA pathway. The BtL pathway with plantation wood achieves a value of 4318 L ha^{-1} $year^{-1}$, the HEFA pathway with the jatropha plant was 3001 L ha^{-1} $year^{-1}$, ethanol from corn was 2992 L ha^{-1} $year^{-1}$, and ethanol from sugar cane was 3653 L ha^{-1} $year^{-1}$. At the lower end of the scale, cotton and HEFA from soy bean achieve productivities of 91 and 699 L ha^{-1} $year^{-1}$, respectively. In ref 3, the authors indicate productivities of 510 L ha^{-1} $year^{-1}$ for a HEFA process based on the conversion of the jatropha plant in Mexico, of 2041 L ha^{-1} $year^{-1}$ for a FT-based conversion of woody biomass in Germany, and of 5263 L ha^{-1} $year^{-1}$ for the FT-based conversion of eucalyptus in Brazil. The order of magnitude of these results is in good agreement with the values derived in ref 49.

In the PtL pathway, liquid hydrocarbon fuels are produced by the Fischer−Tropsch conversion of syngas, where the hydrogen in the syngas is derived from water electrolysis and the carbon monoxide from a reverse water gas shift, which converts carbon dioxide and hydrogen into carbon monoxide and water. The efficiency of this pathway using solar photovoltaic electricity and including energy penalties for carbon dioxide capture and for the mismatch between the photovoltaic and the electrolysis potential is estimated to be 7.7%.[50] The efficiency from electrical energy to chemical energy stored in the FT fuels is determined to be 44.6% in ref 39. With literature data for the specific land requirements of different electricity generation pathways,[51] the area-specific productivity of the power-to-liquid fuel pathway can be estimated. The specific values of land use are 11 m^2 MWh_{el}^{-1} $year^{-1}$ for a parabolic trough plant in Spain[51] and assumed 6 m^2 MWh_{el}^{-1} $year^{-1}$ at a higher irradiation of 2500 kWh m^{-2} $year^{-1}$,[52] 17 m^2 MWh_{el}^{-1} $year^{-1}$ for a solar tower plant in Spain[51] and 8 m^2 MWh_{el}^{-1} $year^{-1}$ at 2500 kWh m^{-2} $year^{-1}$ (own computations), 56 m^2 MWh_{el}^{-1} $year^{-1}$ for a PV plant in Germany,[51] 2.9−72.1 m^2 MWh_{el}^{-1} $year^{-1}$ for a wind farm (lower value: cleared ground area and higher value: totally affected ground area),[53] and 60 m^2 MWh_{el}^{-1} $year^{-1}$ for coal mining (lignite) in Germany.[51] By multiplication with the electricity-to-fuel efficiency of the PtL pathway derived above and by referencing the result to produced liters per hectare and year, area-specific productivities are derived for comparison with the BtL and the solar thermochemical pathway. The results are shown in Figure 6.

Solar thermochemical fuels in the baseline case have an area-specific productivity of 33 362 L of jet fuel-equivalent ha^{-1} $year^{-1}$ and therefore achieve a higher value than some of the power-to-liquid pathways, i.e. those based on electricity from coal combustion, photovoltaics in Germany, and a solar tower in Spain. The reason for the higher value of solar thermochemistry over the PtL pathway with a solar tower in Spain is the higher solar irradiation of the baseline case plant over the location in Spain. The PtL pathway based on coal combustion has a lower productivity than the solar thermochemical fuel pathway due to a relatively high area demand for coal mining in Germany.[51]

The production of biofuels relies on the cultivation of biomass and is therefore based on photosynthesis. The photosynthetical efficiency from sunlight to chemical energy has a theoretical maximum value of 5%[55] but achieves in practice much lower values below 1%.[56] Since the conversion efficiency directly translates into the required cultivation area, in general higher values are noted for biofuels. The preferred areas of biomass cultivation are located in mild and humid climate zones, while the best locations for solar fuels are found in arid climate zones with high solar irradiation. Biofuels and solar fuels therefore do not compete for the same land and could be implemented complementarily. The solar thermochemical fuel pathway therefore achieves area-specific productivities on the same order of magnitude as electrochemical pathways, where for both the final values depend on the specific assumptions made, e.g., the primary energy source or plant location.

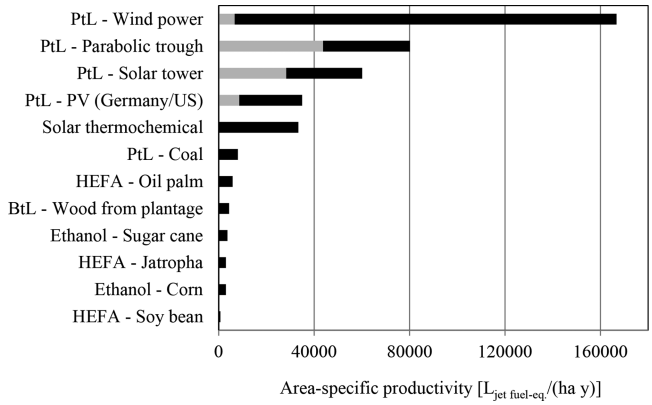

Figure 6. Area-specific productivities of the solar thermochemical fuel pathway in comparison with biomass-based pathways (BtL, HEFA, and ethanol; sources 3 and 49) and power-to-liquid pathways (PtL, based on different sources of electricity: 50−54 and our own computations). The results are given in liters of jet fuel equivalent per hectare per year, where the conversion is done on an energy basis (LHV). The gray and black bars denote the actually covered land area (gray) and the totally affected land area for wind power (black), plants in Spain (gray) and under a higher solar resource of 2500 kWh m^{-2} y^{-1} (black) for solar trough and tower, and plant locations in Germany (gray) and the United States (black) for solar PV. The assumptions are ideal conditions for plant growth of the biomass-based pathways and favorable developments of the thermochemical conversion efficiency and the energy penalty of carbon dioxide capture for the solar thermochemical pathway.

4. SENSITIVITY STUDY

In the following, deviations of the nonstoichiometry and the cycle time with respect to the baseline case assumed in the calculations above shall be discussed. The ambitious target of 0.1 for the nonstoichiometry per cycle of the reactive material ceria is relaxed, where a value of 0.031 is achieved in experiments today.[24] In the same experiment, the cycle time is 30 min, which gives a total of 16 cycles per day, assuming an operation time of 8 h. The fuel production per mass is then proportional to the nonstoichiometry times the number of cycles per day. At a constant plant output of the baseline case, a lower fuel productivity leads to an increase of the amount of ceria. Because the water footprint is the specific water demand per liter of jet fuel, i.e. the total water demand divided by the amount of fuel produced, it is proportional to the fuel productivity. In Figure 7, the water footprint is shown as a function of the nonstoichiometry times the number of cycles per day. A decrease of fuel productivity strongly increases the

DOI: 10.1021/acs.est.7b02633
Environ. Sci. Technol. 2017, 51, 12938−12947

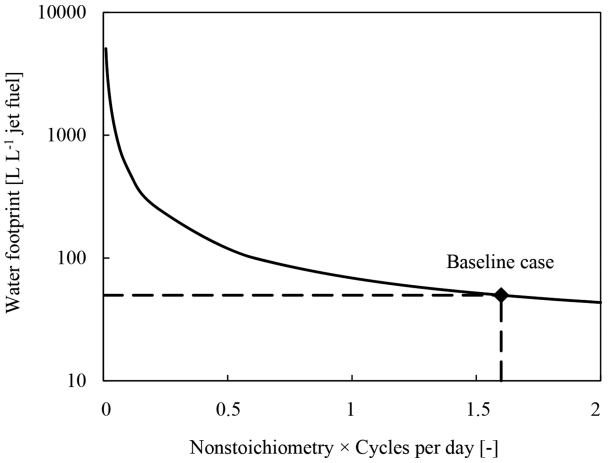

Figure 7. Water footprint as a function of nonstoichiometry of the reactive material times the number of cycles per day. The conditions of the baseline case (a nonstoichiometry of 0.1 and 16 cycles per day) are indicated, resulting in a water footprint of 49.8 liters per liter of jet fuel.

water footprint because, proportionally, a larger amount of ceria is required, which is associated with a large water demand for its provision. A lower nonstoichiometry of 0.031 leads to a required mass of ceria of 22 522 tons, compared to 6982 tons in the baseline case. The water footprint then rises from 49.8 to 120.1 liters per liter of jet fuel. The reaction conditions of the thermochemical fuel production thus have a strong influence on the water demand of the cycle, where a lower nonstoichiometry can in principle be compensated by a shorter cycle time. However, it should be noted that the increased demand of water occurs at the location of ceria mining and not at the plant location. Furthermore, even the assumption of reduced nonstoichiometry leads to a water footprint that is still significantly lower than that of fuels based on the conversion of biomass.

A variation of the irradiation level leads to a proportional change of the area-specific fuel productivity, i.e., the construction of the plant at a location with a 10% higher DNI increases the fuel productivity by an equal 10%. The water footprint, however, changes only slightly because the solar concentration facility is resized to provide a constant power input to the reactors and the specific water footprint of the concentration facility is low.

AUTHOR INFORMATION

Corresponding Author

*Phone: +49-89-307484939; fax: +49-89-307484920; e-mail: christoph.falter@bauhaus-luftfahrt.net.

ORCID

Christoph Falter: 0000-0002-8860-7100

Notes

The authors declare no competing financial interest.

ACKNOWLEDGMENTS

We gratefully acknowledge the contributions of Paul Koltun, Valentin Batteiger, and Arne Roth. The research leading to these results has received funding from the European Union's Seventh Framework Program (FP7/2007-2013) under grant agreement no. 285098, Project SOLAR-JET, and from the European Union's Horizon 2020 research and innovation program under grant agreement no. 654408.

REFERENCES

(1) Kuhn, H.; Falter, C.; Sizmann, A. Renewable Energy Perspectives for Aviation. *Proc. 3rd CEAS Air Conf. 21st AIDAA Congr.* **2011**, 1249−1259.

(2) Falter, C.; Batteiger, V.; Sizmann, A. Climate Impact and Economic Feasibility of Solar Thermochemical Jet Fuel Production. *Environ. Sci. Technol.* **2016**, *50* (1), 470−477.

(3) Gröngröft, A.; Meisel, K.; Hauschild, S.; Grasemann, E.; Peetz, D.; Meier, K.; Roth, A.; Riegel, F.; Endres, C. *Abschlussbericht Projekt BurnFAIR*; Deutsche Lufthansa: Berlin, Germany, 2014.

(4) Stratton, R. W.; Wong, H. M.; Hileman, J. I. *Life cycle gas emissions from alternative jet fuels*; PARTNER Project 28 report; Report number Partner-Coe-2010-001; Partnership for AiR Transportation Noise and Emissions Reduction: Cambridge, MA, 2010.

(5) Berninghausen, C. Power-to-fuel http://ecosummit.net/uploads/eco12_220312_1515_carlberninghausen_sunfire.pdf (accessed May 17, 2016).

(6) Chueh, W. C.; Falter, C.; Abbott, M.; Scipio, D.; Furler, P.; Haile, S. M.; Steinfeld, A. High-flux solar-driven thermochemical dissociation of CO_2 and H_2O using nonstoichiometric ceria. *Science* **2010**, *330* (6012), 1797−1801.

(7) Steinfeld, A.; Epstein, M. Light Years Ahead. *Chem. Br.* **2001**, *37* (5), 30−32.

(8) Kim, J.; Henao, C. A.; Johnson, T. A.; Dedrick, D. E.; Miller, J. E.; Stechel, E. B.; Maravelias, C. T. Methanol production from CO_2 using solar-thermal energy: process development and techno-economic analysis. *Energy Environ. Sci.* **2011**, *4* (9), 3122.

(9) Kim, J.; Johnson, T. a.; Miller, J. E.; Stechel, E. B.; Maravelias, C. T. Fuel production from CO_2 using solar-thermal energy: system level analysis. *Energy Environ. Sci.* **2012**, *5* (9), 8417.

(10) Graf, D.; Monnerie, N.; Roeb, M.; Schmitz, M.; Sattler, C. Economic comparison of solar hydrogen generation by means of thermochemical cycles and electrolysis. *Int. J. Hydrogen Energy* **2008**, *33*, 4511−4519.

(11) Kim, J.; Miller, J. E.; Maravelias, C. T.; Stechel, E. B. Comparative analysis of environmental impact of S2P (Sunshine to Petrol) system for transportation fuel production. *Appl. Energy* **2013**, *111*, 1089−1098.

(12) United Nations. *Water Security & the Global Water Agenda*; The United Nations University: Hamilton, Canada, 2013.

(13) United Nations. *UN water scarcity fact sheet*; United Nations: New York, NY, 2013.

(14) Furler, P.; Scheffe, J.; Marxer, D.; Gorbar, M.; Bonk, A.; Vogt, U.; Steinfeld, A. Thermochemical CO_2 splitting via redox cycling of ceria reticulated foam structures with dual-scale porosities. *Phys. Chem. Chem. Phys.* **2014**, *16* (22), 10503−10511.

(15) American Society for Testing and Materials (ASTM). *D7566-10a, Standard Specification for Aviation Turbine Fuel Containing Synthesized Hydrocarbons*; ASTM: West Conshohocken, PA, 2010, 1−20.

(16) Sargent & Lundy. *Assessment of Parabolic Trough and Power Tower Solar Technology; SL-5641*; Sargent & Lundy: Chicago, IL, 2003.

(17) Climeworks. Capturing CO_2 from Air. *Manuf. Green Fuels from Renew. Energy Work. DTU Risø, Roskilde, 14 April 2015*; Climeworks: Zurich, Switzerland, 2015.

(18) Heath, G. A.; Burkhardt, J. J.; Turchi, C. S. *Life Cycle Environmental Impacts Resulting from the Manufacture of the Heliostat Field for a Reference Power Tower Design in the United States*; SolarPACES: Marrakech, Morocco, **2012**; pp 6−12.

(19) Whitaker, M. B.; Heath, G. a; Burkhardt, J. J.; Turchi, C. S. Life Cycle Assessment of a Power Tower Concentrating Solar Plant and the Impacts of Key Design Alternatives. *Environ. Sci. Technol.* **2013**, *47* (11), 5896−5903.

(20) Shell Global Solutions. Pearl GtL. http://www.shell.com/about-us/major-projects/pearl-gtl.html (accessed January 1, 2014).

(21) Geerlings, H. Shell Global Solutions, The Hague, The Netherlands. *Personal communication*, 2014.

DOI: 10.1021/acs.est.7b02633
Environ. Sci. Technol. 2017, 51, 12938−12947

(22) Raluy, G.; Serra, L.; Uche, J. Life cycle assessment of MSF, MED and RO desalination technologies. *Energy* **2006**, *31* (13), 2361−2372.
(23) Hoekstra, A. Y.; Chapagain, A. K.; Aldaya, M. M.; Mekonnen, M. M. *The Water Footprint Assessment Manual*; Earthscan Ltd.: London, Washington, D.C., 2011.
(24) Marxer, D.; Furler, P.; Takacs, M.; Steinfeld, A. Solar thermochemical splitting of CO_2 into separate streams of CO and O_2 with high selectivity, stability, conversion, and efficiency. *Energy Environ. Sci.* **2017**, *10* (5), 1142−1149.
(25) Furler, P.; Scheffe, J.; Gorbar, M.; Moes, L.; Vogt, U.; Steinfeld, A. Solar thermochemical CO_2 splitting utilizing a reticulated porous ceria redox system. *Energy Fuels* **2012**, *26* (11), 7051−7059.
(26) Institute for Applied Ecology. Gemis. http://iinas.org/gemis-de.html. Darmstadt, Germany 2008.
(27) Koltun, P.; Tharumarajah, A. Life Cycle Impact of Rare Earth Elements. *ISRN Metall.* **2014**, *2014*, 1−10.
(28) Browning, C.; Northey, S.; Haque, N.; Bruckard, W.; Cooksey, M. Life Cycle Assessment of Rare Earth Production from Monazite. In *REWAS 2016*; Springer International Publishing: Cham, Switzerland, 2016; Vol. *14*, pp 83−88.
(29) Haque, N.; Hughes, A.; Lim, S.; Vernon, C. Rare Earth Elements: Overview of Mining, Mineralogy, Uses, Sustainability and Environmental Impact. *Resources* **2014**, *3* (4), 614−635.
(30) Häring, H. W.; Ahner, C. *Industrial Gases Processing*; Wiley VCH Verlag GmbH & Co. KgaA: Weinheim, Germany, 2008.
(31) Wurzbacher, J. A.; Gebald, C.; Piatkowski, N.; Steinfeld, A. Concurrent separation of CO_2 and H_2O from air by a temperature-vacuum swing adsorption/desorption cycle. *Environ. Sci. Technol.* **2012**, *46* (16), 9191−9198.
(32) Gebald, C.; Wurzbacher, J. A.; Tingaut, P.; Zimmermann, T.; Steinfeld, A. Amine-based nanofibrillated cellulose as adsorbent for CO_2 capture from air. *Environ. Sci. Technol.* **2011**, *45* (20), 9101−9108.
(33) Wurzbacher, J. A.; Gebald, C.; Steinfeld, A. Separation of CO_2 from air by temperature-vacuum swing adsorption using diamine-functionalized silica gel. *Energy Environ. Sci.* **2011**, *4* (9), 3584.
(34) Climeworks LLC. CO_2 air capture demonstration plant. http://www.climeworks.com/co2-capture-plants.html (accessed June 1, 2014).
(35) Beiermann, D. Development of an Upgrading Model and Application to XtL Processes Integration of the upgrading unit into the BtL process chain. In *Proc. DGMK/SCI Conf*; DGMK: Hamburg, Germany, **2007**; pp 199−206.
(36) Zeman, F. Energy and material balance of CO_2 capture from ambient air. *Environ. Sci. Technol.* **2007**, *41* (21), 7558−7563.
(37) Milnes, M. The mathematics of pumping water. http://www.raeng.org.uk/education/diploma/maths/pdf/exemplars_advanced/17_pumping_water.pdf (accessed January 1, 2013).
(38) Trieb, F.; Schillings, C.; O'Sullivan, M.; Pregger, T.; Hoyer-Klick, C. *Global potential of concentrating solar power*; SolarPACES: Marrakech, Morocco, 2009.
(39) König, D. H.; Freiberg, M.; Dietrich, R.-U.; Wörner, A. Techno-economic study of the storage of fluctuating renewable energy in liquid hydrocarbons. *Fuel* **2015**, *159*, 289−297.
(40) Mekonnen, M. M.; Gerbens-Leenes, P. W.; Hoekstra, A. Y. The consumptive water footprint of electricity and heat: a global assessment. *Environ. Sci. Water Res. Technol.* **2015**, *1* (3), 285−297.
(41) US Department of Energy. *Energy Demands on Water Resources*. Report to Congress on the Interdependency of Energy and Water; U.S. Department of Energy: Washington, D.C., 2006.
(42) Wu, M.; Mintz, M.; Wang, M.; Arora, S. Water consumption in the production of ethanol and petroleum gasoline. *Environ. Manage.* **2009**, *44* (5), 981−997.
(43) Vera-Morales, M.; Schäfer, A. *Final Report: Fuel-Cycle Assessment of Alternative Aviation Fuels*; University of Cambridge Institute for Aviation and the Environment: Cambridge, U.K., 2009.
(44) Dominguez-Faus, R.; Powers, S. E.; Burken, J. G.; Alvarez, P. J. The water footprint of biofuels: A drink or drive issue? *Environ. Sci. Technol.* **2009**, *43* (9), 3005−3010.
(45) Mekonnen, M.; Hoekstra, A. *The Green, Blue and Grey Water Footprint of Crops and Derived Crop Products*; Main Report, Value of Water Research Report Series No. 47; UNESCO-IHE: Paris, France, 2010, *2* (47), 1−1196.
(46) Gerbens-Leenes, W.; Hoekstra, A. Y.; van der Meer, T. H. The water footprint of bioenergy. *Proc. Natl. Acad. Sci. U. S. A.* **2009**, *106* (25), 10219−10223.
(47) Yang, J.; Xu, M.; Zhang, X.; Hu, Q.; Sommerfeld, M.; Chen, Y. Life-cycle analysis on biodiesel production from microalgae: Water footprint and nutrients balance. *Bioresour. Technol.* **2011**, *102* (1), 159−165.
(48) Don Hofstrand. Liquid Fuel Measurements and Conversions. http://www.extension.iastate.edu/agdm/ (accessed January 1, 2015).
(49) Riegel, F. Das nachhaltige Potenzial von Flüssigkraftstoffen aus Biomasse: Eine globale Abschätzung auf der Basis von hochaufgelösten Geodaten, Dissertation, submitted, Ludwig-Maximilians-Universität München, 2014.
(50) Haije, W.; Geerlings, H. Efficient Production of Solar Fuel Using Existing Large Scale Production Technologies. *Environ. Sci. Technol.* **2011**, *45* (20), 8609−8610.
(51) European Academies Science Advisory Council. *Concentrating solar power: its potential contribution to a sustainable energy future*; European Academies Science Advisory Council: Halle, Germany, 2011.
(52) Eberle, M. K. *Sonnenkraft aus der Steckdose - Concentrating Solar Power (CSP) − eine Renaissance*; ETH Zürich: Treffpunkt Science City, 2010, 2010.
(53) McDonald, R. I.; Fargione, J.; Kiesecker, J.; Miller, W. M.; Powell, J. Energy Sprawl or Energy Efficiency: Climate Policy Impacts on Natural Habitat for the United States of America. *PLoS One* **2009**, *4* (8), e6802.
(54) Brown, P.; Whitney, G. U.S. *Renewable Electricity Generation: Resources and Challenges*; Congressional Research Service: Washington, D.C., **2011**.
(55) Hall, D. O.; Rao, K. K. *Photosynthesis*, 6th ed.; Cambridge University Press: Cambridge, U.K., 1999.
(56) Blankenship, R. E.; Tiede, D. M.; Barber, J.; Brudvig, G. W.; Fleming, G.; Ghirardi, M.; Gunner, M. R.; Junge, W.; Kramer, D. M.; Melis, A.; et al. Comparing photosynthetic and photovoltaic efficiencies and recognizing the potential for improvement. *Science* **2011**, *332* (6031), 805−809.

DOI: 10.1021/acs.est.7b02633
Environ. Sci. Technol. 2017, 51, 12938−12947